Origin of the pattern of trabecular bone: An experiment and a model

Zbisław Tabor,[1,*] Eugeniusz Rokita,[1,2] and Tadeusz Cichocki[3]
[1]*Department of Biophysics, Collegium Medicum, Jagiellonian University, Grzegórzecka 169, 31-531, Cracow, Poland*
[2]*Institute of Physics, Jagiellonian University, Cracow, Poland*
[3]*Department of Histology, Collegium Medicum, Jagiellonian University, Cracow, Poland*
(Received 15 February 2002; published 13 November 2002)

As a result of an experiment in which the development of a mineral phase in the rabbit embryo was observed, a model is proposed to explain the mechanism that controls the place of precipitation of crystals in mineralizing tissue. The reaction-diffusion equations for the specified compounds are formulated and solved. Among a variety of compounds the concentrations of carbon dioxide, oxygen, HCO_3^- ions, H^+ ions, calcium, and inorganic phosphorus are evaluated. CO_2, HCO_3^- ions, and H^+ ions, are distinguished due to their key role in the maintenance of the *p*H value. The local concentration of oxygen is the pivot factor that controls the metabolic rate, i.e., production of CO_2. Next the supersaturation was estimated on the basis of the calculated values of *p*H and the concentrations of calcium and inorganic phosphorus. It is assumed that the synthesis of the organic matrix breaks the metastable equilibrium with respect to spontaneous precipitation and leads to the deposition of minerals. It was found that the geometry of the vasculature determines the shape of primitive trabecular bone (woven bone) while the value of the diffusion coefficient may be the key factor indicating the possibility of mineralization under the control of a living organism.

DOI: 10.1103/PhysRevE.66.051906 PACS number(s): 87.19.−j

INTRODUCTION

Despite many years of intensive research a convincing quantitative description of the mechanism of bone tissue formation does not exist. Bone mineral metabolism has been associated with a temporally and spatially self-organized system, and it has been suggested that some spatiotemporal behavior of a reaction-diffusion model related to this metabolism could be responsible for the patterning of the trabecular architecture of embryonic bone [1–3]. Studies of the formation of bone tissue are not progressing successfully, however, mainly due to difficulties in the *in situ* approach. The majority of the results collected so far originate from *in vitro* experiments including cell cultures, from histochemical findings (at light and electron microscopic levels), and from biochemical analysis of body fluids. It is commonly accepted [4,5], however, that the final stage of bone tissue formation comprises the precipitation of an inorganic phase on the scaffold of an organic matrix. In the embryonic skeleton, the woven (primary) bone is formed first, followed by its remodeling and formation of mature bone as the skeleton develops.

The primary bone is always laid down as a network of trabeculae (primary spongiosa). The processes that determine the shape of woven bone and chemical composition of its minerals remain poorly understood. *In vitro* studies have shown that, depending on the applied experimental conditions (degree of supersaturation, *p*H, duration of the reaction, concentrations of other ions and biomolecules, chemical form of the seeds) different Ca-P compounds may be involved in woven bone mineralization [6–8]. Studies of the internal architecture of woven bone are not so advanced. Probably the shape of woven bone is a result of complex interactions between genetic and physicochemical factors. On the basis of the data collected so far we are not able, however, to point out a pivot factor responsible for the deposition of minerals at given sites of primary spongiosa.

In the present paper the influence of the tissue vascularization on woven bone architecture is investigated. An experiment was performed in which the development of a mineral phase in the rabbit embryo was observed and a model is proposed to explain the mechanism that controls the place of precipitation of crystals in mineralizing tissue. The results of the experiment are compared with the results of model calculations. Possible implications of the model are indicated.

MODEL

The proposed model describes the initial ossification that mostly occurs in the embryonic skeleton. A careful examination of the published data [9,10] indicates that three parameters play a key role in the formation of bone minerals. They are the concentrations of calcium and inorganic phosphorus in the interstitial fluid and the *p*H value at the place of mineral precipitation. It should be clearly pointed out that the list of organic and inorganic factors that have been postulated to be involved in the mineralization process is very long [11–13]. In many cases contradictory results are reported. However, with the use of the above-mentioned parameters, thorough control of the precipitation of different Ca-P compounds from the solution is possible.

Since the minerals are deposited extracellularly in close association with certain components of the organic matrix [14], formation of the organic matrix has to precede the deposition of minerals. In the model the primitive connective tissue is treated as the ''organic matrix'' which delivers a scaffold for mineral deposition.

The concentration $\rho(x,y,z,t)$ of each compound within the primary ossification center (POC) has to satisfy the diffusion equation

*Corresponding author. Email address: tabor@alphas.if.uj.edu.pl

$$\frac{\partial \rho}{\partial t} - D\nabla^2 \rho = \text{production}(t) - \text{consumption}(t), \qquad (1)$$

where D is the coefficient of diffusion. Since the formation of bone minerals is much slower than the time required for diffusion of molecules over a distance equal to the separation of two blood vessels in the POC (hours vs seconds), stationary solutions (i.e., $\partial\rho/\partial t = 0$) of Eq. (1) are considered in the model. Additionally, the considerations are limited to two-dimensional (2D) space since the verification of the calculations will be performed for 2D, bone sections.

Among a variety of compounds whose concentrations in the POC are described by Eq. (1), oxygen, carbon dioxide, HCO_3^-, H^+, calcium, and inorganic phosphorus concentrations are considered. It is assumed that the concentrations at the boundaries surrounding the POC and the concentrations in the blood do not differ by more than 1%. To avoid problems with unknown flows generated by the blood vessels present in the POC [i.e., an unknown production term in Eq. (1)], boundaries are created around the blood vessels and the values of concentrations at these boundaries are set equal to the concentrations in blood. The concentrations of oxygen, carbon dioxide, HCO_3^-, H^+, calcium, and inorganic phosphorus in blood are equal to 1.3×10^{-4}, 1.2×10^{-3}, 2.4×10^{-2}, 4×10^{-8}, 1.1×10^{-3}, and 0.9×10^{-3} mol/l, respectively [15]. Physically dissolved O_2 and CO_2 as well as ionized calcium were considered.

Keeping in mind that oxygen is only consumed in the body, Eq. (1) for the oxygen concentration $\rho_O(x,y)$ reduces to

$$-D_o\nabla^2\rho_o = -F(\rho_o), \qquad (2)$$

where D_O is the diffusion coefficient for O_2. The function $F(\rho_O)$ describes the oxygen-consumption–oxygen-concentration curve. In the model only the gross features of the curve are important. The intermediate details of oxygen consumption are not considered. In agreement with reported data [16], it is assumed that at low O_2 concentration the consumption of O_2 increases linearly with oxygen concentration, i.e., $F(\rho_O)=C\rho_O$, while above that concentration the rate of consumption remains constant, i.e., $F(\rho_O)=C_0$. It can be estimated on the basis of total body oxygen consumption that the value of C is in the range from 5×10^{-5} to 5×10^{-2} s^{-1} [16]. C_0 was found using this C value and assuming that the critical concentration of oxygen at which the consumption begins to drop amounts to 8×10^{-5} mol/l [16].

Although the metabolic processes within the POC comprise various biochemical reactions, which are interconnected and affect one another, production of CO_2 is considered only as the end product of oxygen consumption. Each disappearing mole of oxygen produces one mole of carbon dioxide. CO_2 is distinguished in the model due to its key role in the maintenance of pH value. The buffering capacity of interstitial fluid is lower than that of plasma as a result of lower protein content and depends mainly on its bicarbonate buffer system. Dissolved CO_2 in the interstitial fluid is hydrated to form carbonic acid while the carbonic acid, in turn, dissociates into hydrogen ions and bicarbonate ions according to

$$H_2O + CO_2 \underset{d_{HCO}}{\overset{d_{CO}}{\rightleftarrows}} H^+ + HCO_3^-, \qquad (3)$$

where d_{CO} and d_{HCO} are the reaction rates. The concentrations of CO_2 $[\rho_{CO}(x,y)]$, HCO_3^- $[\rho_{HCO}(x,y)]$, and H^+ $[\rho_H(x,y)]$ satisfy the three coupled equations

$$-D_{CO}\nabla^2\rho_{CO} = F(\rho_O) + d_{HCO}\rho_{HCO}\rho_H - d_{CO}\rho_{CO}, \qquad (4)$$

$$-D_{HCO}\nabla^2\rho_{HCO} = -d_{HCO}\rho_{HCO}\rho_H + d_{CO}\rho_{CO}, \qquad (5)$$

$$-D_H\nabla^2\rho_H = -d_{HCO}\rho_{HCO}\rho_H + d_{CO}\rho_{CO}, \qquad (6)$$

where D_{CO}, D_{HCO}, and D_H are the diffusion coefficients for CO_2, HCO_3^-, and H^+, respectively. By taking the logarithm of ρ_H the pH value is calculated:

$$p\text{H} = -\log_{10}(\rho_H). \qquad (7)$$

The concentrations of calcium $[\rho_{Ca}(x,y)]$ and inorganic phosphorus P_i $[\rho_{P_i}(x,y)]$ are described by two equations:

$$-D_{Ca}\nabla^2\rho_{Ca} = -F_{Ca}(\rho_{Ca},\ldots), \qquad (8)$$

$$-D_{P_i}\nabla^2\rho_{P_i} = -F_{P_i}(\rho_{P_i},\ldots), \qquad (9)$$

where D_{Ca} and D_{P_i} are the diffusion coefficients for Ca and P_i, respectively. The functions F_{Ca} and F_{P_i} describe the consumption of Ca and P ions as a result of the inorganic deposit formation in woven bone. In the model the concentrations of Ca and P before the onset of mineral precipitation are described, i.e., $F_{Ca}=0$ and $F_{P_i}=0$.

To quantify the ability to precipitation, the supersaturation (σ) was defined as

$$\sigma = \frac{\kappa - \kappa_E(p\text{H})}{\kappa_E(p\text{H})}, \qquad (10)$$

where κ is the ionic product of ρ_{Ca} and ρ_{P_i} and $\kappa_E(p\text{H})$ is the solubility constant. To describe the influence of the pH value on κ_E, the relationship of the product of total calcium and phosphate concentrations and pH values of solutions saturated with respect to hydroxyapatite [17] was approximated using the formula

$$\log_{10}[\kappa_E(p\text{H})] \approx 16.5 - 5.5(p\text{H}) + 0.28(p\text{H})^2. \qquad (11)$$

The free parameters that the model depends on are the diffusion coefficient for oxygen D_O (it may depend on the density inside the POC) and the reaction rates of the reaction (3), i.e., d_{CO} and d_{HCO} (these parameters are controlled, for example, by carbonic anhydrase, present in erythrocytes, which speeds up the carbonic acid reaction by a factor of $\sim10^4$ [18]). The diffusion coefficients for CO_2, HCO_3, H^+, Ca, and P_i are calculated with the use of D_O and the Stokes-Einstein relation $[D\sim1/(\text{molecular weight})^{1/3}]$.

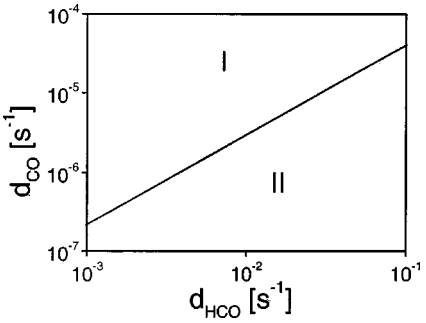

FIG. 1. The phase diagram for the solutions of a simplified version of the model. In region I a minimum and in region II a maximum of the supersaturation appears between the blood vessels. The input parameters are $D_O = 10^2\ \mu m^2\ s^{-1}$ and $C = 0.01\ s^{-1}$. For abbreviations see text.

In the following a system with two blood vessels in the POC was considered to examine the influence of the values of the parameters on the solution of the model equations. In this simple version of the model the following values of the free parameters were tested: the value of D_O ranges from 1 to $10^4\ \mu m^2/s$ [19], while the parameters d_{CO} and d_{HCO} range between 10^{-7} and $10^{-1}\ s^{-1}$. The POC was selected as a $300 \times 300\ \mu m^2$ square. The blood vessels were placed on the diagonal (positions $x_1 = y_1 = 100\ \mu m$ and $x_2 = y_2 = 200\ \mu m$).

Depending on the values of the relative rates of the processes involved in the reaction (3), supersaturation may decrease (Fig. 1, region I) or increase (Fig. 1, region II) outside the blood vessels. These different σ distributions are presented in Fig. 2. The increase of the σ value radically changes the precipitation and growth of Ca-P compounds. Generally, the supersaturation of body fluids with Ca-P compounds may be considered as the dominant variable controlling the rate of mineral deposition [17,20–23]. This is true both for spontaneous nucleation and for precipitation induced by inoculating with seeds (heterogeneous nucleation). Therefore, it may be stated that, if growth of supersaturation is observed when moving away from the blood vessels, the most favorable conditions for mineral precipitation appear at the centerpoint between two blood vessels. This observation is in agreement with reported data [5] concerning the localization of minerals in woven bone. It must be noted, however, that body fluids contain a variety of substances that are known to impede crystal growth [24,25]. Thus the net precipitation probability may depend not only on supersaturation but also on the concentration of mineralization inhibitors, not considered in the study.

Next the influence of the diffusion coefficients on the properties of the model was examined. It should be noted that the POC is treated in the model as a homogeneous mixture of cells and organic substances. Bundles of collagen fibrils embedded in the gel-like extracellular matrix run in all directions. The regular parallel pattern of collagen fibers characteristic for mature bone is not observed in woven bone. Moreover, the chemical interaction of the compounds under consideration with the POC matrix was not included in the calculations. Therefore the transport of the compounds is approximated as an isotropic, concentration gradient dependent process. In a dense material like the collagen matrix, which constitutes a considerable barrier to diffusion, small values of the diffusion coefficients are expected. In contrast, in aqueous solution or in soft materials diffusion is facilitated and the diffusion coefficients are bigger. The results of simulations confirmed that small values of the diffusion coefficients correspond to maxima of σ outside the blood vessels, while an increase of D_O by a factor of $\sim 10^2$ causes the positions of blood vessels and maximum σ to correlate (Fig. 3). A large value of the diffusion coefficient probably represents a physiological situation that takes place in the soft tissues. Therefore, the above results may give an answer to the question, ''Why do not most tissue calcify under normal physiological conditions?''

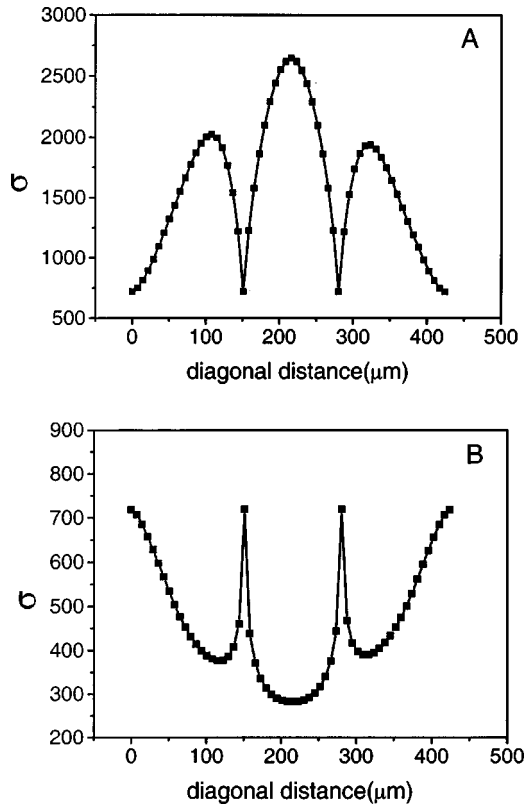

FIG. 2. The values of the supersaturation (σ) across the diagonal of the POC. The two blood vessels are placed at positions ~140 and 280 μm. The input parameters are $D_O = 10^2\ \mu m^2\ s^{-1}$, $C = 0.01\ s^{-1}$, $d_{CO} = 10^{-6}$ (a) and $10^{-5}\ s^{-1}$ (b), and $d_{HCO} = 10^{-2}\ s^{-1}$. For abbreviations see text.

EXPERIMENT

It is very difficult, if not impossible, to verify the model by direct measurements of the compound concentrations *in vivo* in woven bone. Therefore, verification of the model calculations was performed using micrographs of rabbit embryo bone sections.

In the experiment two female rabbits at 21 days of pregnancy were deeply anesthetized with anesthetic drug administrated intraperitoneally and afterward bled out by cutting the aorta. The fetuses were removed, killed under anesthesia

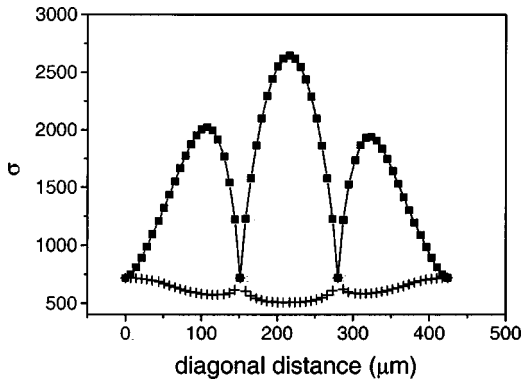

FIG. 3. The precipitation blockage induced by an increase of the value of the diffusion coefficients in the POC. The input parameters are $D_O=10^2$ (squares) and 10^4 μm^2 s^{-1} (crosses), $C=0.01$ s^{-1}, $d_{CO}=10^{-6}$ s^{-1}, and $d_{HCO}=10^{-2}$ s^{-1}. The two blood vessels are placed at positions ~140 and 280 μm. For abbreviations see text.

by cutting off the heart apex, and perfused through the ascending aorta with heparine supplemented saline to wash out the blood. Next, black ink with 5% gelatin was injected until the mucous membranes (conjunctiva) turned black. Altogether ten fetuses were investigated. The lower limbs were dissected, fixed in 7% formalin, then washed, paraffin embedded in the routine way, cut into 10 μm thin sections, and stained with hematoxilin-eosin. From all the samples 13 sections were cut (depending on the material size) and selected for further analysis. The places of active bone formation at the head parts of the femurs were investigated. In all cases the blood vessels showed up black and were easily identified. For each section 3–4 two-dimensional images were acquired, using a microscope connected to a digital camera. A typical image of mineralizing tissue is presented in Fig. 4. An excellent presentation of techniques developed for visualization and quantification of vessels in bone was published recently by Barou *et al.* [26].

Digital images of the mineralizing tissue specimens enable the precise determination of the woven bone and blood vessel architecture. The positions of the blood vessels extracted from the micrograph were used to determine the

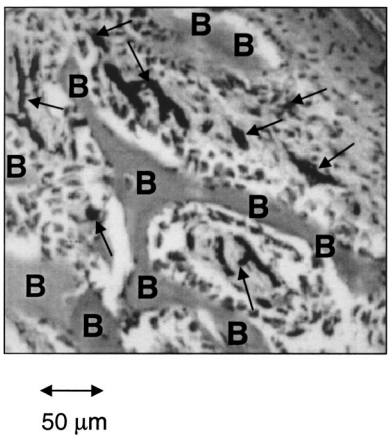

FIG. 4. Section of the rabbit embryo bone. Black arrows indicate blood vessels. "B" denotes the deposits of minerals.

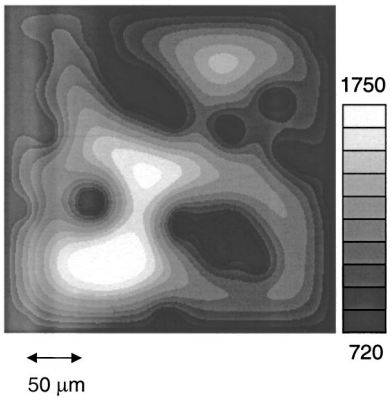

FIG. 5. The distribution of the degree of supersaturation. There is a good correlation between the mineralized trabeculae depicted in Fig. 4 and the value of supersaturation. Close to the blood vessels the values are lowest. The input parameters are $D_O=10^2$ μm^2 s^{-1}, $C=0.01$ s^{-1}, $d_{CO}=2\times10^{-6}$ s^{-1}, and $d_{HCO}=10^{-2}$ s^{-1}. For abbreviations see text.

boundary conditions in a POC selected as a 300×300 μm^2 square. The model equations were solved using standard techniques for elliptic equations [27] and the distribution of the supersaturation was evaluated according to Eq. (10). An example of a supersaturation calculation based on the blood vessel geometry depicted in Fig. 4 is presented in Fig. 5. The values of the model parameters used in the calculations are listed in the figure caption. This is a set of values of the parameters for which an increase of supersaturation is observed when moving away from the blood vessels (as was discussed in the previous section).

From a comparison of Figs. 4 and 5 it follows that for the proper choice of values of the model parameters the distribution of the supersaturation evaluated from the model equations reproduces the distribution of the mineral deposits. We have found that the Turing mechanism of pattern generation is not necessary to explain the origin of the structure of trabecular bone. It should be pointed out that the observed agreement between the supersaturation and mineral deposit distributions is only indirect proof of the correctness of the model. In fact, the experiment tests the connection between the geometry of the vasculature and the calculated distribution of supersaturation. The results of the comparison seem to be encouraging. Other results that follow from the model (i.e., the role of reaction rates and diffusion coefficients) remain experimentally unchecked. However, the observed distribution of minerals as well as the fact that they are deposited extracellularly strongly suggests that the geometry of woven bone is determined by a diffusion-involving process. Then, based on the accepted physicochemical knowledge concerning the precipitation of bone minerals the choice of supersaturation as the quantity steering mineral deposition is natural. From the comparison of micrographs and model calculations it also seems that this choice could be the proper one.

When comparing measured and simulated distributions it should be kept in mind that the micrograph is a section of the 3D structure. Therefore the vessels that run in close vicinity

but parallel to the section plane are not included in the calculation but could in fact change the bone geometry.

DISCUSSION

The mechanism responsible for woven bone mineralization may work as follows. Carbon dioxide is produced in the POC as it is in other tissues. However, removal of the carbon dioxide is more difficult from the POC than it is from soft tissues due to the low coefficients of diffusion in the POC [19]. By this mechanism the body keeps the *p*H within the POC higher than that of the other body compartments. This is a purely physicochemical process. Moreover, the constants that control the reaction (3) amount to values from region II of the phase diagram (it is in general possible that the values of these constants are, as in blood, cell metabolism dependent). Therefore, the concentrations of oxygen, HCO_3, H^+, Ca, and P_i decrease while the concentration of carbon dioxide and the *p*H increase if the distance from the blood vessel grows. Comparison of the distributions of the Ca and P_i concentrations with the κ_E distribution confirms unequivocally that changes of the κ_E value compensate, in excess, the decrease of the concentrations of Ca and P_i ions. This means that the interstitial fluid in the POC becomes supersaturated and the precipitation of Ca-P minerals is facilitated. It should be noted that the supersaturation correlates with the distance from the vessel. Changes of the *p*H value in the POC that correspond to an increase of σ by approximately 100% do not surpass $\sim$0.5 units. Such changes are well tolerated by living organisms [15].

The above-tested model is based on some simplifying assumptions. First, the precipitation of minerals in the body was treated as a purely physicochemical process, controlled entirely by concentrations of Ca and P ions and *p*H value. During the deposition of inorganic substances within the organic matrix, the inorganic and organic components can interact and can set up special relationships. The organic matrix induced processes are not included in the model. Secondly, we were not able to calculate precisely the influence of *p*H on the precipitation of a Ca-P compound from the interstitial fluid. The estimation was performed using the solubility diagrams for an *in vitro* system that simulates the physiological conditions [17]. It should be pointed out that the model describes the initial physicochemical conditions inside the POC, before ossification begins. The appearance of mineralization centers destroys the homogeneity of the tissue and the model equations have to be modified.

CONCLUSIONS

On the basis of the model calculations it was shown that blocking the diffusional pathways in bone tissue could regulate inorganic phase formation. Then the most favorable physicochemical conditions for woven bone formation appear outside the blood vessels. Thus the pattern of primary bone reflects the architecture of the blood vessel network. A mechanism for the physicochemical control of the primary bone formation process based on a reaction-diffusion model was proposed.

[1] J. F. Staub, P. Tracqui, S. Lausson, G. Milhaud, and A. M. Perault-Staub, Bone (N.Y.) **10**, 77 (1989).
[2] J. F. Staub, P. Tracqui, P. Brezillon, G. Milhaud, and A. M. Perault-Staub, Am. J. Physiol. **254**, R134 (1988).
[3] B. Courtin, A. M. Perault-Staub, and J. F. Staub, Acta Biotheor. **43**, 373 (1995).
[4] J. A. Buckwalter, M. J. Glimcher, R. R. Cooper, and R. Recker, Int. Course Lect. **45**, 371 (1996).
[5] D. W. Fawcett, *A Textbook of Histology* (Chapman and Hall, New York, 1994).
[6] B. D. Boyan, Z. Shwartz, and A. L. Boskey, Bone (N.Y.) **27**, 341 (2000).
[7] A. L. Boskey, J. Dent. Res. **76**, 1433 (1997).
[8] W. J. Landis, Connect. Tissue Res. **34**, 239 (1996).
[9] W. E. Brown and L. C. Chow, J. Cryst. Growth **53**, 31 (1981).
[10] Y. L. Chang, C. M. Stanford, and J. C. Keller, J. Biomed. Mater. Res. **52**, 270 (2000).
[11] G. R. Mundy, Growth Regul. **3**, 124 (1993).
[12] A. L. Boskey, J. Cell Biochem. Suppl. **30-31**, 83 (1998).
[13] G. Karsenty, Matrix Biol. **19**, 85 (2000).
[14] M. J. Glimcher, Biomaterials **11**, 7 (1990).
[15] W. C. Bowman and M. J. Rand, *Textbook of Pharmacology* (Blackwell Scientific, Oxford, 1980).
[16] N. Rashevsky, *Mathematical Biophysics* (Dover, New York, 1962).
[17] P. G. Koutsokos and G. H. Nancollas, J. Cryst. Growth **53**, 10 (1981).
[18] J. F. Nunn, *Applied Respiratory Physiology* (Butterworth-Heineman, Boston, 2000).
[19] E. P. Katz, Biochim. Biophys. Acta **194**, 121 (1969).
[20] H. E. Lungader Madsen and F. Christensson, J. Cryst. Growth **114**, 613 (1991).
[21] G. Vereecke and J. Lemaitre, J. Cryst. Growth **104**, 820 (1990).
[22] M. T. Fulmer, I. C. Ison, C. R. Hankermayer, B. R. Constantz, and J. Ross, Biomaterials **23**, 751 (2002).
[23] A. A. Baig, J. L. Fox, Z. Wang, W. I. Higuchi, S. C. Miller, A. M. Barry, and M. Otsuka, Calcif. Tissue Int. **64**, 329 (1999).
[24] G. K. Hunter, P. V. Hauschka, A. R. Poole, L. C. Rosenberg, H. A. Goldberg, Biochem. J. **317**, 59 (1996).
[25] R. C. Crowther, C. M. Pritchard, S. M. Qiu, and R. D. Solway, Liver **13**, 141 (1993).
[26] O. Barou, S. Mekraldi, L. Vico, G. Boivin, C. Alexandre, and M. H. Lafage-Proust, Bone (N.Y.) **30**, 604 (2002).
[27] W. H. Press, S. A. Teukolsky, W. T. Vetterling, and B. P. Flannery, *Numerical Recipes* (Cambridge University Press, Cambridge, England, 1995).